A. Plumtree and S. Schäfer**

Initiation and Short Crack Behaviour in Aluminium Alloy Castings

REFERENCE Plumtree, A. and Schäfer, S., **Initiation and Short Crack Behaviour in Aluminium Alloy Castings**, *The Behaviour of Short Fatigue Cracks*, EGF Pub. 1(Edited by K. J. Miller and E. R. de los Rios) 1986, Mechanical Engineering Publications, London, pp. 215–227.

ABSTRACT The initiation and early growth of fatigue cracks in strain cycled squeeze-formed aluminium–7% silicon alloy castings have been investigated using single-stage replication techniques. Cracks initiated at the silicon particles in the interdendritic region, generally at triple points. Cracking of the silicon particles took place together with debonding of the aluminium–silicon interface at high cyclic strains, whereas at the low strain ranges only the latter took place. In all cases, fatigue cracks propagated through the interdendritic regions.

The critical length of a short fatigue crack was directly related to the dendrite spacing; cracks of about twice this length and less displayed initially fast growth rates. At high cyclic strains they continued to grow at a constant rate. At low cyclic strains the cracks experienced deceleration until they passed through the first triple points in the interdendritic regions after initiation. Subsequently they accelerated to blend with the crack growth rate for long cracks. This crack growth behaviour was explained in terms of larger plastic strains existing at the tips of short cracks when compared to long cracks.

Introduction

The behaviour of short fatigue cracks has been described as 'anomalous' because the propagation rate does not correspond to that seen for long cracks. For the latter, the log. crack propagation rate is a linear function of log. crack length. In contrast, short fatigue cracks demonstrate different types of propagation behaviour, namely, acceleration, deceleration to crack arrest, or deceleration followed by acceleration. Long cracks do not propagate at levels below the threshold stress intensity factor range (ΔK_{th}), whereas it is known that short cracks grow below this level (**1**)(**2**). In fact, it is debatable whether linear elastic fracture mechanics (LEFM) is applicable to short cracks.

One attractive model for the prediction of propagation rates of short fatigue cracks based on crack tip strains has been propounded by Lankford (**2**) and developed by de los Rios *et al.* (**3**). This model allows for arrest, deceleration followed by subsequent acceleration, and continuous acceleration of short cracks. It includes the effect of grain boundary retardation of short fatigue cracks and is based on a larger plastic strain range at the tips of short cracks when compared with long cracks. The size of the crack-tip plastic zone is of the order of half the crack length (**4**). As the small crack grows and approaches a grain boundary or another barrier, the crack propagation rate will be reduced if crack-tip slip is restricted by this obstacle. The continued growth of the small crack requires the propagation of crack-tip slip into neighbouring grains.

* Department of Mechanical Engineering, University of Waterloo, Waterloo, Ontario, Canada.

The present work was undertaken to investigate the short fatigue crack growth behaviour in a squeeze-formed aluminium alloy and to examine the results in terms of the crack-tip slip model.

Experimental procedure

A commercial squeeze-formed aluminium–7% silicon casting alloy was used for the testing programme. The alloy conformed to British specification L99, which is similar to the Aluminum Association A356 designation. The material was heat-treated to the T-6 condition resulting in a 0.2 per cent offset yield stress of 256 MPa and ultimate tensile strength of 342 MPa.

Completely reversed strain controlled uniaxial cyclic testing ($R = -1$) was carried out at room temperature on smooth cylindrical specimens of 5 mm diameter with a gauge length of 14 mm. A sinusoidal waveform was used at frequencies between 0.1 Hz and 20 Hz. All tests were conducted on an MTS servo-controlled closed-loop electrohydraulic testing machine.

Fatigue crack propagation rates were determined using replication techniques. This also permitted a critical evaluation of crack initiation sites and crack propagation paths to be made. The replicas were examined using a JEOL JSM-840 scanning electron microscope (SEM).

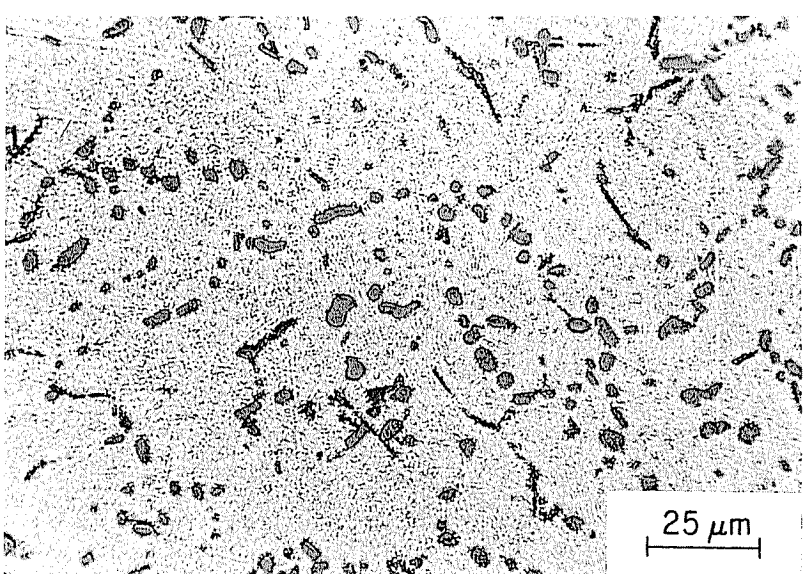

Fig 1 General microstructure of the squeeze-formed aluminium–7% silicon alloy. Etched with 5% HF in water

Results

The results of the cyclic strain-life tests allowed the relationship between total true strain range ($\Delta\varepsilon_T$) and number of reversals to failure ($2N_F$) to be expressed as follows

$$\Delta\varepsilon_T = 0.057(2N_f)^{-0.40} + 0.018(2N_f)^{-0.12} \quad (1)$$

The first term on the right-hand side of equation (1) is the plastic strain component and the second, the elastic component of total strain range.

During each test the stress response was monitored continually. For the lowest strain range employed ($\Delta\varepsilon_T = 0.36$ per cent) the stress range at half life (1×10^6 cycles) was 250 MPa.

The microstructures consisted of primary aluminium-rich dendrites surrounded by an interdendritic eutectic consisting of silicon particles (dark grey) and the aluminium-rich α-phase, as shown in Fig. 1. The dendrite spacing ranged between 25 μm and 45 μm. On strain cycling, crack initiation was associated with the silicon particles, and in particular those present at triple points of the interdendritic network. Figure 2 shows a silicon particle intact before fatigue testing and which cracked after 100 cycles at a total strain range of 1.0 per cent. Besides fracture of the silicon particles, debonding occurred at the high strain ranges, as also seen in Fig. 2. At the low strain ranges cracks

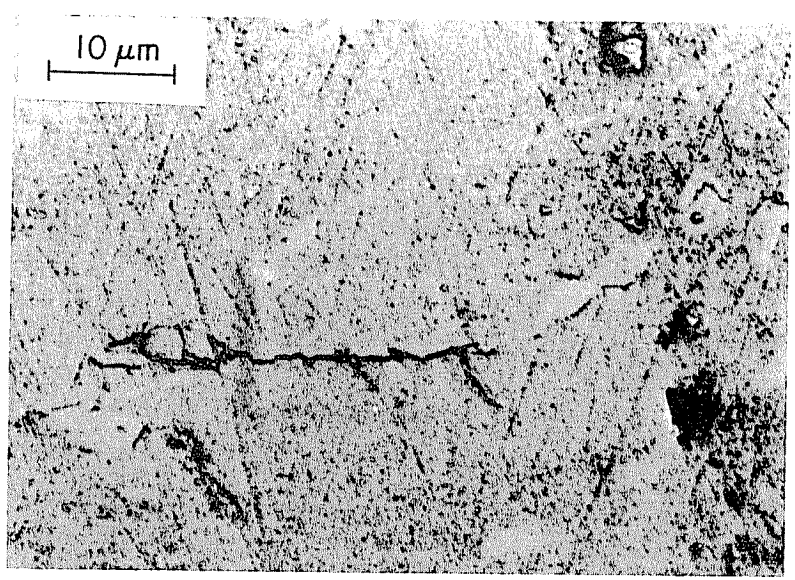

Fig 2 Fracture of silicon particle (indicated by arrow) as consequence of strain cycling at $\Delta\varepsilon_T = 1$ per cent after 80% life with stress response of 270 MPa. Also note fracture and debonding of other silicon particles

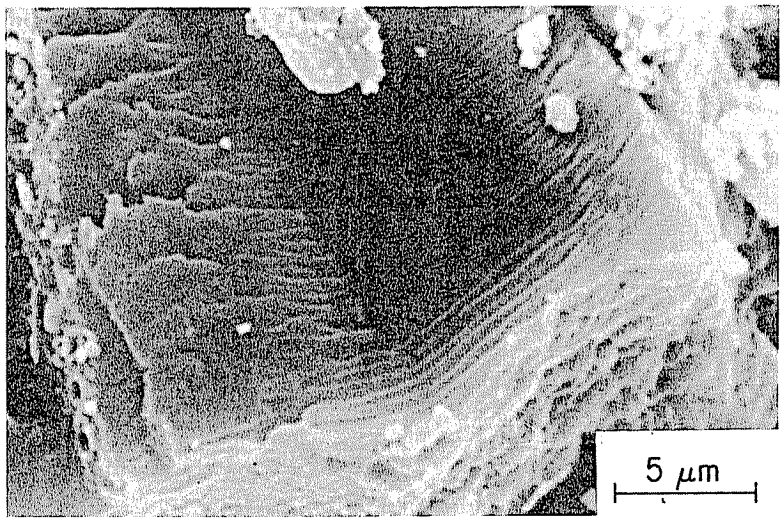

Fig 3 Fatigue fracture of eutectic aluminium in interdendritic region

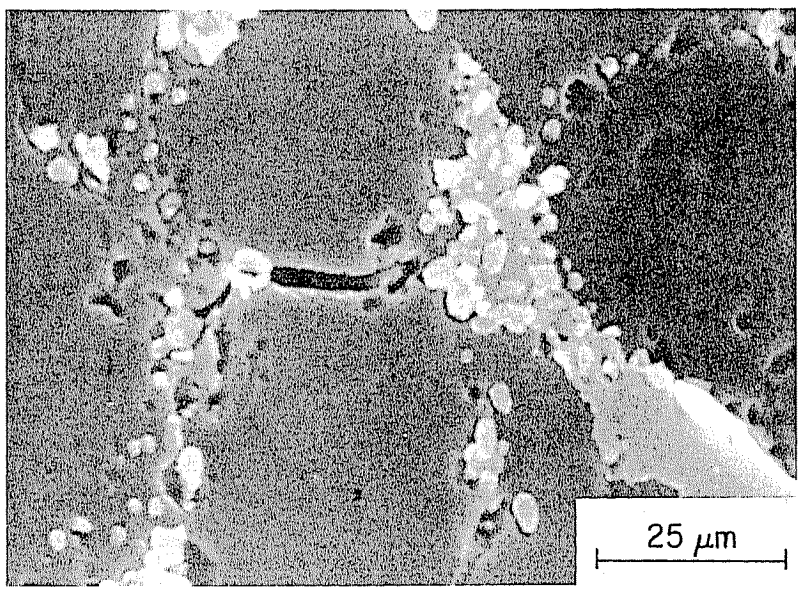

Fig 4 Short crack held at first triple points after initiation. Etched with 5% HF in water

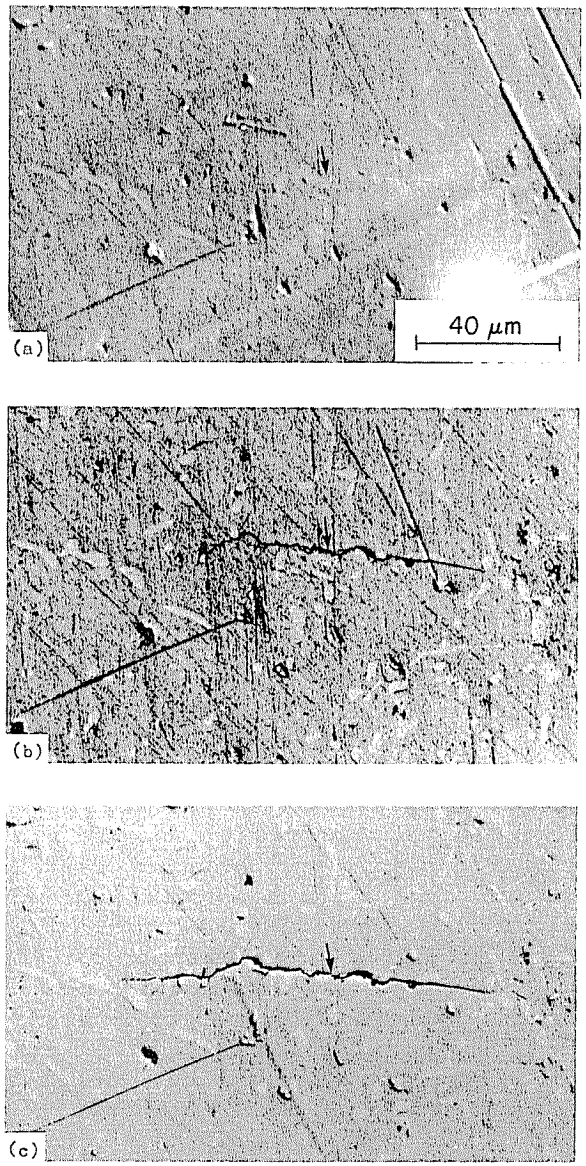

Fig 5 Surface crack development. Crack originated at triple point indicated by arrow
(a) 50 per cent life (b) 65 per cent life (c) 80 per cent life

formed by interfacial decohesion between the silicon particles and the matrix. Once initiated, the cracks progressed by fatigue failure through the eutectic α-aluminium in those parts of the interdendritic areas where silicon particles were not present. Figure 3 shows transgranular fracture which has occurred in the eutectic aluminium within this interdendritic region.

In general, cracks were found to be macroscopically transverse to the stress axis, yet microscopically they meandered a considerable amount. The cracks followed the eutectic areas rather than cutting directly through the primary aluminium-rich dendrites and this is illustrated in Fig. 4. A small interdendritic crack is seen which has grown until it reached the first triple points and then stopped.

The evolution of the catastrophic surface crack from initiation to final fracture is given in Fig. 5. These replica photographs show the crack at various stages in the fatigue life. The light coloured areas are silicon particles. No crack is visible in Fig. 5(a), which represents the surface of the specimen after 10^6 cycles. After 1.3×10^6 cycles a crack initiated at an interdendritic triple point and grew to a length of less than twice the triple point spacing, as seen in Fig. 5(b). It is important to note that the right side of the crack is held at the first triple point, after initiation, in the interdendritic network. After a further 0.3×10^6 cycles the crack grew to a length of two triple point spacings by progressing to the nearest triple point on the left side (Fig. 5(c)). No further growth had obviously taken place past the triple point on the right side. This specimen finally fractured after 2×10^6 cycles, indicating a rapid crack growth rate during the remaining 0.4×10^6 cycles.

The surface crack propagation rate (dl/dN) can be approximated by using the secant method (**5**)

$$dl/dN = \Delta l/\Delta N \qquad (2)$$

A log–log plot of dl/dN vs l, given in Fig. 6 shows the representative growth behaviour of fatigue cracks for low and high strains. The short cracks displayed anomalous behaviour. For low strains, a decrease in dl/dN was observed as the cracks approached the first triple points in the interdendritic network after initiation. In the majority of cases, since the cracks originated at interdendritic triple points, the minimum crack growth rate corresponded to two interdendritic facets. Once these triple points were overcome, the cracks accelerated and eventually their surface crack propagation rate became the same as that for long cracks. On the other hand, at high strains, the short cracks grew faster than those at the low strains yet they displayed a relatively constant or slightly increasing growth rate until they blended with the long crack growth behaviour.

In order to compare the present work on aluminium alloys with that of other workers, such as Lankford (**2**) who use stress intensity range factors (ΔK), it was necessary to convert the surface crack lengths (l) to crack depths (a) and express the results in terms of ΔK. Pearson (**6**) measured the shape of a fatigue crack initiated at a second phase particle from a plane surface in aluminium

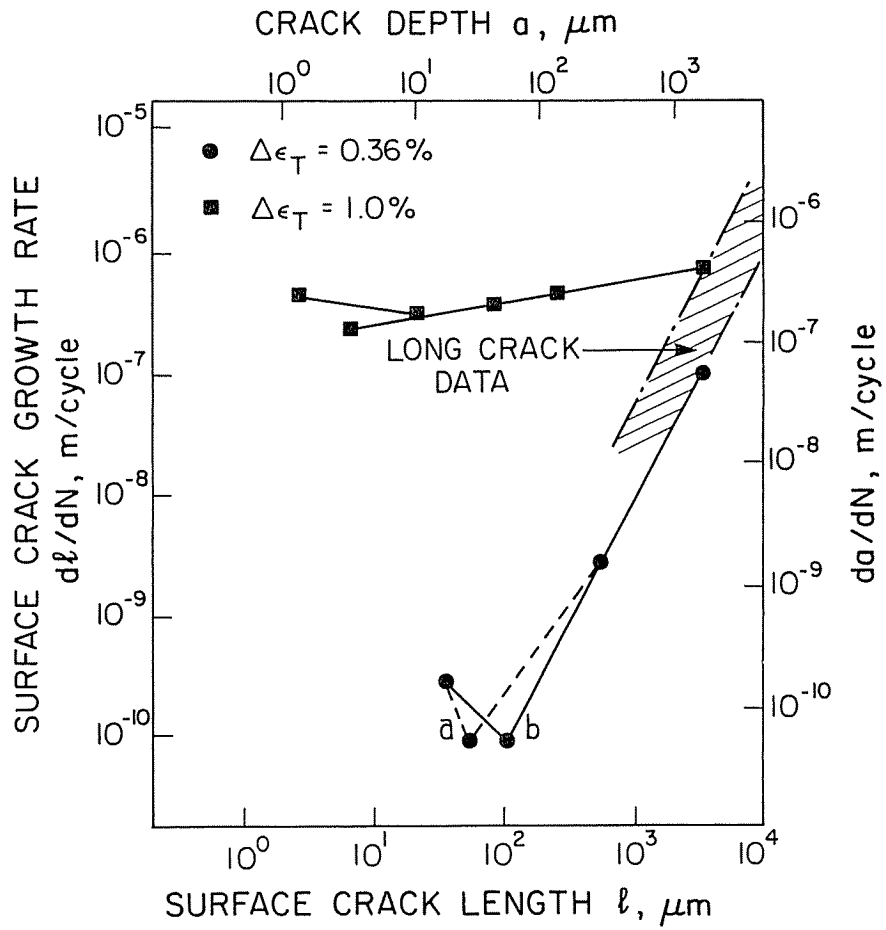

Fig 6 Variation of crack rate with crack length. Curve (a) represents cracks which have initiated between interdendritic triple points, whereas curve (b) represents those which have started at triple points

alloy and found that the crack, which had a 400 μm surface length, was approximately semi-circular in shape. Dowling (**7**) has reported that for axially loaded smooth specimens of approximately the same size as those used in this investigation, the crack depth was 'approximately equal to half the surface length' for all cracks examined. These cracks were between 250 μm and 1800 μm in surface length. Thus, it is taken that $a = l/2$ and this relationship is used for the plots involving crack depths in Figs 6 and 7.

By applying both the edge correction factor (**8**) and the approximation for an

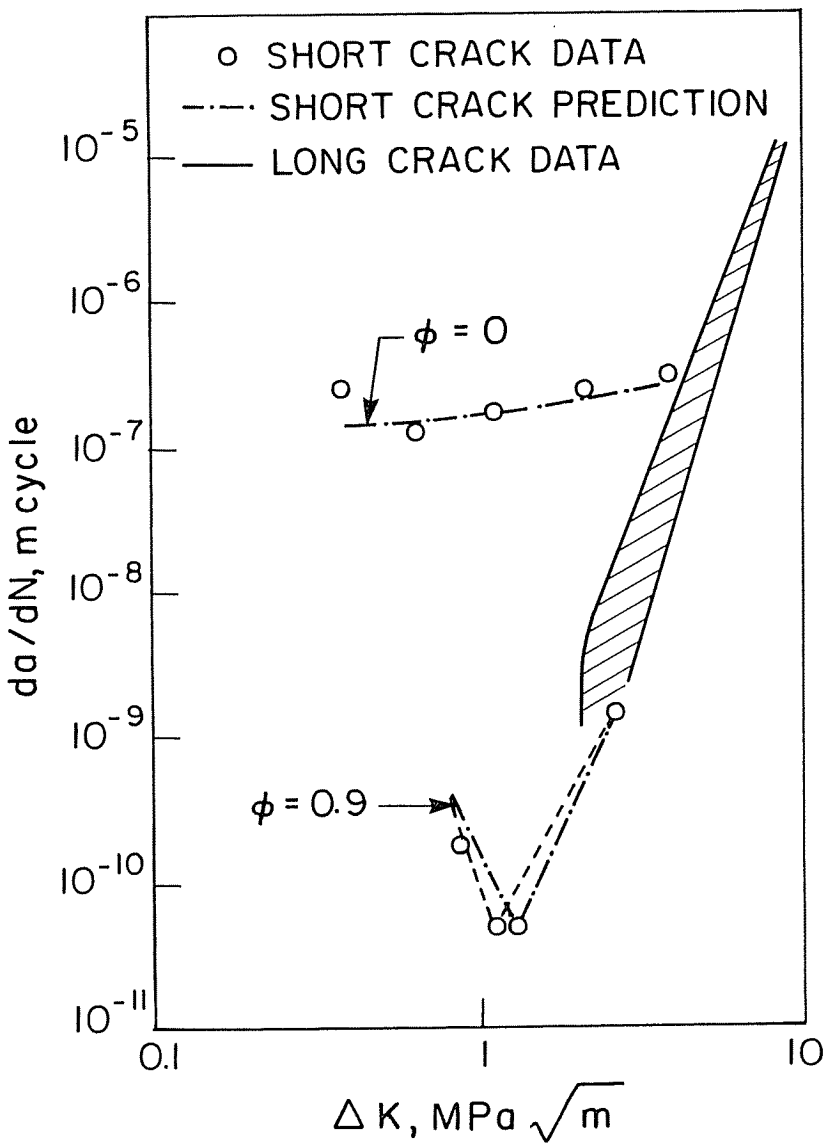

Fig 7 Application of the crack-tip strain model to the representative crack growth curves

embedded circular crack (**9**), and assuming that there are no crack closure effects so that the crack is open when the nominal applied load is tensile and closed when the applied load is compressive, the stress intensity factor range may be expressed by:

$$\Delta K = 0.713\sigma_t\sqrt{(\pi a)} \quad (3)$$

where σ_t is the applied tensile stress and da/dN is the mean crack depth corresponding to a. It should be noted that for the fully-reversed tests performed here, $\sigma_t = \Delta\sigma/2$. Thus, the crack propagation rate can be related to the fracture mechanics quantity ΔK at the midpoint of the crack growth interval.

The tensile stress σ_t may be determined from the hysteresis loops plotted during cyclic testing. The results of the calculations of da/dN and ΔK are plotted in Fig. 7 which includes a linear least squares regression for all of the long crack data in the form of the Paris law ($da/dN = C(\Delta K)^m$). The equation of the line is given by

$$da/dN = 4.7 \times 10^{-11}\Delta K^{5.8} \text{ (m/cycle)} \quad (4)$$

The long crack data tend towards a threshold stress intensity factor range near 2 MPa$\sqrt{m}$. This is similar to the threshold of 2 MPa$\sqrt{m}$ reported by Lankford for 7075-T651 (**2**).

Also included in Fig. 7 are the short crack results, which are emphasized by broken lines. The short crack results indicate two different types of behaviour depending upon strain range. For those specimens cycled at high strains, fatigue crack growth occurs at stress intensities below ΔK_{th}, and the cracks accelerate slowly and merge into long crack results. At the low strains, the cracks decelerate until they reach the first barriers. This is equivalent to one or two interdendritic facets depending on the position of the crack initiation site. Once these barriers are overcome, the cracks accelerate, as shown by the broken lines connecting the data points. This type of behaviour is predicted by the crack-tip plastic strain model for fatigue crack growth of short cracks.

Discussion

A number of fracture processes have been identified. These include decohesion between silicon particles and the aluminium-rich α-phase, cleavage of silicon particles, and striated growth of the aluminium-rich phase. Cracks grew preferentially through the eutectic rather than through primary aluminium dendrites. Failure of silicon particles took place when the cyclic stress amplitude was about 270 MPa, representing the stress response of the specimens cycled at high strains of $\Delta\varepsilon_T = 1.0$ per cent. Debonding between the aluminium-rich phase and the silicon particles occurred at both low and high strain ranges.

In general, the mechanism of crack propagation and hence crack growth rate depends on the micro-morphology of the material. In high strength aluminium

alloys at low crack growth rates, the crack path usually follows the interface between inclusions and the matrix. At higher growth rates, inclusions may fracture ahead of the crack front (due to the larger plastic zone size) and cause ductile tearing of the aluminium matrix surrounding the inclusion (**10**). Similar effects can be found in other aluminium casting alloys. Fracture has been observed to occur by interfacial fracture between the aluminium rich phase and silicon particles in both hypereutectic (**11**) and hypoeutectic (**12**) aluminium–silicon alloys.

De los Rios *et al.* (**3**) have developed a shear model involving crack-tip plastic strains to describe the initial crack growth stages, taking into account the location, path and obstacles which must be surmounted. In this manner the initial high crack growth rate of small cracks and subsequent deceleration as they approached crystallographic barriers was represented for a fully annealed 0.4% C steel cycled in torsion. The crack growth rate (da/dN) could be expressed as follows

$$da/dN = f(2\pi aD)^{1/2}\{1 - \phi(D - X)/D\}^3\tau/\mu \tag{5}$$

where f is a constant for the material, τ is half the stress range in torsion, μ the shear modulus, D is the distance from barrier to barrier, X is the total distance from the crack tips to the nearest barrier, and ϕ is a function of the relative crystallographic orientation between neighbouring grains or barriers through which the crack must pass. For instance, when ϕ is formulated in terms of the resolved shear stress (τ) along slip bands in neighbouring grains A and B, then $\phi = 1 - (\tau_B/\tau_A)$, assuming that the crack develops in grain A and propagates into grain B. The maximum value for ϕ is unity and represents the most unfavourable case for crack advance, resulting in arrest. The minimum value for ϕ is zero and is tantamount to no barrier to the crack being present since the orientation in each grain would be the same. Using this model, it has been shown that small cracks are either arrested ($\phi = 1$) or temporarily halted ($0 < \phi < 1$) depending upon stress level (**3**).

In the present work a similar effect was seen. At the high strains no decrease in growth rate of the small cracks was observed because the corresponding stress level was sufficiently high to overcome the barriers to crack advance, yet at low strains significant deceleration in the small cracks was observed as they approached these barriers. Unfortunately the model of de los Rios *et al.* (**3**) cannot be applied directly because the constant f has not been determined independently for aluminium alloys. However it is possible to apply a similarly based model which has been verified for these alloys. This is the model of Lankford (**2**). The concepts of a larger plastic strain range $\Delta\varepsilon_p$ associated with the tip of a small crack, grain boundary blockage of crack tip slip, and the same low cycle fatigue crack tip failure process established for large cracks, have been combined (**13**) into a crack growth expression for small cracks, i.e.

$$\frac{da}{dN} = \frac{\Delta aC}{\Delta\varepsilon_p(0)}\Delta K^{n'}[1 - \phi\{(D - X)/D\}^m] \tag{6}$$

where C and n' are experimentally measured constants describing the ΔK dependence of the strain at microcrack tips far from grain boundaries; m also is an experimentally established constant related to the rate at which the strain decreases as a boundary or barrier is approached, $\Delta\varepsilon_p(0)$ is the accumulated plastic strain at the crack tip, and Δa is an increment of crack advance. The other terms have been defined previously.

The available experimental data for $m(=2)$ and $n'(=0.2)$ have been applied to the present work. Since no measured values for Δa and $\Delta\varepsilon_p(0)$ were available, a constant C_1 has been introduced such that

$$C_1 = \frac{\Delta a}{\Delta\varepsilon_p(0)}\,C \tag{7}$$

Hence equation (6) becomes

$$\frac{da}{dN} = C_1\Delta K^{0.2}[1 - \phi\{(D - X)/D\}^2] \tag{8}$$

The values of ϕ can be deduced from the shape of the log da/dN vs log ΔK plot and these are included in Fig. 7. For the high strains $\phi = 0$, with the consequence that there was no impediment to crack growth since the associated stress response was sufficient to continue crack-tip slip past the triple points. On the other hand for the low strains $\phi = 0.9$, indicating a strong barrier to short crack growth. In this case, the distance between barriers, D, was either one or two interdendritic spacings, respectively, depending whether the crack initiated between interdendritic nodes (as in Fig. 4) or at an interdendritic node (as in Fig. 5). Hence equation (8) appears to be applicable to the present results. For specific use of equation (8), however, C_1 takes on different numerical values according to the strain range, i.e., $C_1 = 1.7 \times 10^{-7}$ for $\Delta\varepsilon_T = 1.0$ per cent and $C_1 = 5.8 \times 10^{-10}$ for $\Delta\varepsilon_T = 0.36$ per cent. This is to be expected since both Δa and $\Delta\varepsilon_p(0)$ depend upon strain range. In particular, it indicates that the increment of crack advance, Δa, is greater for the higher strain range.

Figures 6 and 7 show that the minimum growth rate for short cracks at the low strain range occurs when the crack depths, a, are approximately 25 μm and 45 μm. Above the larger critical value, LEFM analysis may be considered. The limiting case would result in an equivalent crack depth, a_0, which may be calculated for the present set of experimental conditions by rearranging equation (3) in the following manner

$$a_o = \left(\frac{\Delta K_{th}}{0.713\Delta\sigma_o}\right)^2\frac{1}{\pi} \tag{9}$$

where ΔK_{th} is the threshold and $\Delta\sigma_o$ is the endurance limit (= 125 MPa for 2×10^6 cycles). From Fig. 7, if ΔK_{th} is taken as 2 MPa$\sqrt{m}$ then a_o is 80 μm. If ΔK_{th} is taken as 1.1 MPa$\sqrt{m}$, then a_o is 48 μm, which is approximately the equivalent of two interdentritic spacings. This value has strong metallurgical implications since ΔK_{th} and $\Delta\sigma_o$ may be influenced by thermo-mechanical

treatment, as well as by surface preparation and testing conditions. However when the crack depth is less than a_0, short crack growth behaviour should be expected, whereas when $a > a_0$ short crack growth would not be expected. These effects were observed in the present investigation.

Conclusions

(1) Fatigue cracks in a squeeze-formed aluminium–silicon alloy casting have been observed to initiate at silicon particles either by debonding at the interface with the aluminium matrix or by cracking of the silicon particles. The former is associated with low cyclic strain ranges and long lives.

(2) Crack growth occurred preferentially in the interdendritic regions rather than through the dendrites.

(3) Short crack growth behaviour may be expressed using a model based on crack-tip plasticity where the barriers are triple points in the interdendritic regions. These barriers are significant at low strain ranges. In this case, as the short cracks approach the first triple point after initiation, the growth rate is drastically reduced and on overcoming these barriers the cracks accelerate rapidly to eventually comply with the long crack behaviour.

Acknowledgements

The authors would like to thank GKN Technology Ltd, Wolverhampton, UK, for providing the squeeze-formed aluminium alloy. One of the authors, S. Schäfer, wishes to acknowledge the Natural Sciences and Engineering Research Council of Canada (NSERC) for a Scholarship. This work was financed through grants from GKN Technology Ltd, and NSERC.

References

(1) TAYLOR, D. and KNOTT, J. F. (1981) Fatigue crack propagation behaviour of short cracks; the effect of microstructure, *Fatigue Engng Mater. Structures*, **4**, 147–155.

(2) LANKFORD, J. (1983) Material aspects of crack tip yielding and subcritical crack growth in engineering materials, *Mechanical Behaviour of Materials – IV* (Edited by J. Carlsson and N. G. Ohlson), (Pergamon Press, Oxford), Vol. 1, p. 3.

(3) DE LOS RIOS, E. R., MOHAMED, H. J., and MILLER, K. J. (1985) A micromechanics analysis for short fatigue crack growth, *Fatigue Fracture Engng Mater. Structures*, **8**, 49–63.

(4) LANKFORD, J. (1982) The growth of small cracks fatigue cracks in 7075-T6 aluminum, *Fatigue Engng Mater. Structures*, **5**, 233–248.

(5) *Annual Book of ASTM Standards* (1983) Standard Test Method for Constant-Load-Amplitude Fatigue Crack Growth Rates above 10^{-8} m/cycle, ASTM E647–83, 03.01 (American Society for Testing and Materials).

(6) PEARSON, S. (1975) Initiation of fatigue cracks in commercial aluminum alloys and the subsequent propagation of very short cracks, *Engng Fracture Mech.*, **7**, 235–247.

(7) DOWLING, N. E. (1977) Crack growth during low-cycle fatigue of smooth axial specimens, *Cyclic stress–strain and plastic deformation aspects of fatigue crack growth*, STP 637 (American Society for Testing and Materials), p. 97.

(8) BROEK, D. (1983) *Elementary engineering fracture mechanics*, Third revised edition (Martinus Nijhoff, The Hague), p. 77.

(9) BROEK, D. (1983) *Op. cit.*, p. 81.

(10) BROEK, D. (1969) The effect of intermetallic particles on fatigue crack propagation in aluminum alloys, *Fracture 1969* (Edited by P. L. Pratt) (Chapman and Hall, London), p. 734.

(11) CULVER, L. E., RADON, J. C., and BALTHAZAR, J. C. (1984) The influence of silicon on the cyclic crack growth in a cast aluminum alloy, *Life assessment of dynamically loaded materials and structures* (Edited by L. Faria), (National Laboratory of Engineering and Industrial Technology, Lisbon), Vol. 1, p. 495.

(12) OGILVY, I. M. and ROBINSON, P. M. (1975) The fracture of aluminum die casting alloys – the role of morphology and casting defects, 8th SDCE International Die Casting Exposition and Congress, Paper No. G-T75-014 (Society of Die Casting Engineers).

(13) CHAN, K. S. and LANKFORD, J. (1983) A crack tip strain model for the growth of small fatigue cracks, *Scripta. Met.*, **17**, 529–534.